



Published in final edited form as:

Neurogastroenterol Motil. 2010 July ; 22(7): 814–e228. doi:10.1111/j.1365-2982.2010.01487.x.

EXPRESSION AND FUNCTION OF THE BILE ACID RECEPTOR GPBAR1 (TGR5) IN THE MURINE ENTERIC NERVOUS SYSTEM

Daniel P. Poole^{1,3}, Cody Godfrey^{1,3}, Fiore Cattaruzza¹, Graeme S. Cottrell¹, Jacob G. Kirkland^{1,3}, Juan Carlos Pelayo¹, Nigel W. Bunnett^{1,2}, and Carlos U. Corvera^{1,3}

¹Department of Surgery, University of California San Francisco, California

²Department of Physiology, University of California San Francisco, California

³Veterans Affairs Medical Center, San Francisco, California

Abstract

Background—Bile acids (BAs) regulate cells by activating nuclear and membrane-bound receptors. GpBAR1 is a membrane-bound G-protein-coupled receptor that can mediate the rapid, transcription-independent actions of BAs. Although BAs have well-known actions on motility and secretion, nothing is known about the localization and function of GpBAR1 in the gastrointestinal tract.

Methods—We generated an antibody to the C-terminus of human GpBAR1, and characterized the antibody by immunofluorescence and Western blotting of HEK293-GpBAR1-GFP cells. We localized GpBAR1 immunoreactivity (IR) and mRNA in the mouse intestine, and determined the mechanism by which BAs activate GpBAR1 to regulate intestinal motility.

Key Results—The GpBAR1 antibody specifically detected GpBAR1-GFP at the plasma membrane of HEK293 cells, and interacted with proteins corresponding in mass to the GpBAR1-GFP fusion protein. GpBAR1-IR and mRNA were detected in enteric ganglia of the mouse stomach and small and large intestine, and in the *muscularis externa* and mucosa of the small intestine. Within the myenteric plexus of the intestine, GpBAR1-IR was localized to ~50% of all neurons and to >80% of inhibitory motor neurons and descending interneurons expressing nitric oxide synthase. Deoxycholic acid, a GpBAR1 agonist, caused a rapid and sustained inhibition of spontaneous phasic activity of isolated segments of ileum and colon by a neurogenic, cholinergic and nitrenergic mechanism, and delayed gastrointestinal transit.

Conclusions and Inferences—GpBAR1 is unexpectedly expressed in enteric neurons. BAs activate GpBAR1 on inhibitory motor neurons to release nitric oxide and suppress motility, revealing a novel mechanism for the actions of BAs on intestinal motility.

Keywords

Bile acids; G protein-coupled receptor; enteric neurons; motility

Corresponding Author: Carlos U. Corvera, M.D., Veterans Administrative Medical Center Surgical Service (112), Building 200, 4150 Clement Street, San Francisco, California 94121, USA. Tel: 415 221-4810 ext. 4019; Fax: 415 750-2181; carlos.corvera@med.va.gov.

Disclosures: No conflicts of interest exist.

INTRODUCTION

Bile acids (BAs) are essential for the normal digestion and absorption of lipids and vitamins (1). Chenodeoxycholic acid (CDCA) and cholic acid (CA), the two primary BAs in humans, are secreted from the gallbladder into the intestine, and are absorbed and recycled *via* the enterohepatic circulation. The small amounts of primary BAs that reach the colon are dehydroxylated by bacterial enzymes, forming secondary BAs (*e.g.* lithocholic acid [LCA], deoxycholic acid [DCA], tauroolithocholic acid [TLCA], ursodeoxycholic acid [UDCA]). Cholestasis, which is characterized by impaired bile flow into the intestine, is a common feature of acute and chronic liver diseases. The toxic accumulation of BAs in the circulation leads to profound systemic metabolic disturbances by mechanisms that are not fully understood (1).

In addition to their role in digestion, BAs have direct receptor-mediated effects on multiple processes (2,3). Nuclear receptors mediate the delayed actions of BAs that require transcription. BAs activate the farnesoid X receptor (FXR, NR1H4), a nuclear receptor that regulates the expression of biosynthetic enzymes and binding proteins for BAs (4,5). BAs can activate other nuclear receptors, including the pregnane X receptor (PXR) (6) and the vitamin D receptor (7), which protect against the toxic effects of BAs. BAs also rapidly activate signaling pathways and cellular functions that do not require transcription, including cAMP generation, calcium mobilization and activation of protein kinase C and mitogen-activated protein kinases (8–11). G protein coupled bile acid receptor 1 (GpBAR1, also known as TGR5 or M-BAR1) is a membrane-bound G protein-coupled receptor for BAs (12,13). Primary and secondary BAs activate GpBAR1, which couples to adenylyl cyclase and cAMP generation. GpBAR1 is ubiquitous, with the highest expression in brown adipose tissue, placenta, spleen macrophages/monocytes, Kupffer cells, gallbladder and intestine (12–16). Emerging evidence indicates that GpBAR1 controls weight gain and energy expenditure in brown adipose tissue and skeletal muscle by promoting the processing of thyroid hormone (17,18), regulates hepatic microcirculation (16) and chloride secretion in the gall bladder (14), suppresses cytokine release from macrophages (13), and stimulates secretion of glucagon-like peptide (19). However, nothing is known about the localization and function of GpBAR1 in the intestine.

The intestine is exposed to high concentrations of BAs, and BAs have well-described effects on intestinal motility and secretion. BAs stimulate fluid, electrolyte and mucus secretion in the intestine, which may protect against their toxic actions (20–22). BAs also affect intestinal motility, although whether their actions are stimulatory or inhibitory is controversial. *In vivo* studies report that BAs either stimulate motility or have no effect (23–25). Infusion of BAs into the human intestine delays transit, supporting an inhibitory role (26–28). *In vitro* studies show that BAs inhibit contractions of rabbit and guinea pig intestine (29,30). However, the mechanisms by which BAs regulate intestinal function are unknown.

We examined the location and function of GpBAR1 in the mouse gastrointestinal tract. Using a thoroughly characterized GpBAR1 antibody, we made the unexpected observation that GpBAR1 immunoreactivity (IR) is prominently expressed by myenteric inhibitory motor neurons of the intestine. We examined the effects of GpBAR1 agonists on intestinal motility and transit, and determined that BAs inhibit motility by a mechanism that is consistent with activation of GpBAR1 on inhibitory motor neurons that release nitric oxide (NO). We have thereby identified a novel mechanism for the well-known effects of BAs on intestinal motility.

MATERIALS AND METHODS

Animals

Male mice (C57/BL6, 20–25 g, Charles River, Hollister, CA) were killed by sodium pentobarbital injection (200 mg.kg⁻¹, i.p.) and bilateral thoracotomy. The Institutional Animal Care and Use Committee approved all procedures.

Antibodies

New Zealand White rabbits were immunized with a peptide corresponding to the C-terminus of human GpBAR1 with an N-terminal Cys residue for conjugation to keyhole limpet hemocyanin (Cys-P³¹⁰GPSIAYHPSSQSSVDLDLN³³⁰) (Pacific Immunology, San Diego, CA). Rabbits were immunized with 200 µg of conjugated peptide in complete Freund's adjuvant, and were subsequently immunized after each blood collection (2–3 weeks) with 100 µg conjugated peptide in incomplete Freund's adjuvant. Antibody generation was monitored by ELISA using the immunizing peptide. Antibody collected after the fourth and final blood collection was purified by affinity chromatography. Antibody P87/88 was used throughout. Table 1 shows sources and dilutions of other primary antibodies.

Generation of GpBAR1 constructs

Total RNA from human duodenum (5 µg) was reverse transcribed. Primers were designed corresponding to human GpBAR1 (forward 5'-taaagcttatgacgccaacagcactggc-3'; reverse 5'-ttactcgagttagttcaagtcaggctcgac-3'). A construct with green fluorescent protein (GFP) fused to the C-terminus of human GpBAR1 (GpBAR1-GFP) was generated by subcloning into pEGFP-N1 (Clontech, Mountain View, CA). Constructs were confirmed by sequencing.

Generation and maintenance of cell lines

Human embryonic kidney (HEK293) cells were cultured in Dulbecco's modified Eagle's medium supplemented with 10% heat-inactivated fetal bovine serum and zeocin or hygromycin B (100 µg.ml⁻¹). Cells stably expressing human GpBAR1-GFP (HEK-GpBAR1-GFP cells) were generated with the Flp-InTM system (Invitrogen, Carlsbad, CA). In some experiments, cells were transiently transfected with GpBAR1-GFP or empty vector (vector control, VC) using LipofectamineTM 2000 (Invitrogen), and were studied after 48 h.

cAMP generation

Cells were grown to confluency and treated with forskolin (10 nM), BAs (100 µM, Sigma-Aldrich, St. Louis, MO) or vehicle (0.1% ethanol) for 5 min. cAMP was measured by chemiluminescent ELISA (Applied Biosystems Inc., Foster City, CA).

GpBAR1 antibody characterization by immunofluorescence

HEK-GpBAR1-GFP or HEK-VC cells were fixed in 4% paraformaldehyde (0.1 M PBS, pH 7.4, 20 min, 4°C). Cells were washed with PBS containing 0.1% saponin and 1% normal goat serum and incubated with GpBAR1 antibody or GpBAR1 antibody preadsorbed with immunizing peptide (50 µM, overnight, 4°C) (overnight, 4°C). Cells were washed and incubated with goat anti-rabbit Rhodamine Red X (Jackson Immunoresearch, Westgrove, PA; 1:200, 2 h, room temperature). Cells were washed and mounted.

GpBAR1 antibody characterization by Western blotting

Total membranes were prepared from HEK-GpBAR1-GFP or HEK-VC cells. Proteins (25 µg) were separated by SDS-PAGE (12% acrylamide) and transferred to polyvinylidene difluoride membranes (Immobilon-FL, Millipore, Billerica, MA). Membranes were blocked

(Odyssey™ Blocking Buffer, LI-COR Biosciences, Lincoln, NE) and incubated with antibodies to GpBAR1, preadsorbed GpBAR1 or GFP. Membranes were washed and incubated with secondary antibodies conjugated to AlexaFluor®680 (Invitrogen) or IRDye™800 (Rockland Immunochemicals Inc., Gilbertsville, PA; 1:10,000, 1 h, room temperature). Immunoreactive bands were detected by using an Odyssey infrared imaging system.

Detection of GpBAR1 in the mouse gastrointestinal tract by RT-PCR

Total RNA from mouse tissues was treated with DNase I (Ambion, Austin, TX), and reverse transcribed. GpBAR1 was amplified using primers for mouse GpBAR1 (forward, 5'-cactgcccttctctgtcc-3', +537 to +556; reverse, 5'-agttcaggtccagttacgc-3', +985 to +966). To exclude contamination by genomic DNA, control reactions omitted reverse transcriptase. Products were separated by electrophoresis on a 2% gel, detected with ethidium bromide, and sequenced.

GpBAR1 localization in gastrointestinal tissue

To prepare tissue sections, mouse tissues were fixed in 4% paraformaldehyde (overnight, 4°C), cleared with dimethyl sulfoxide and PBS washes (3 × 10 min), and incubated in 30% sucrose PBS (overnight, 4°C). Tissues were embedded in Optimal Cutting Temperature compound (Tissue-Tek, Sakura Finetek, Torrance, CA) and sectioned (10–12 μm). Sections were incubated in PBS containing 10% normal horse serum and 0.1% Triton X-100 (1 h, room temperature). Sections were then incubated with primary antibodies (overnight, 4°C), washed, incubated with donkey anti-rabbit, -chicken or -goat IgG conjugated to Rhodamine Red X or FITC (Jackson; 1:200, 1 h, room temperature), and mounted. To prepare whole mounts, intestine was placed in cold PBS containing nicardipine (1 μM) to inhibit smooth muscle contraction. The intestine was opened, fixed with 4% paraformaldehyde (overnight, 4°C), and whole mount dissections were made of the longitudinal muscle-myenteric plexus and submucosa-submucosal plexus (31). Tissue was then processed for indirect immunofluorescence.

Confocal Microscopy

Specimens were observed by using a Zeiss LSM510 META confocal system. Images were collected at 1024 × 1024 pixel resolution using Zeiss objectives (Plan-Neofluar 40× NA 1.3; Fluor Plan Aplanachromat 63×, NA 1.4; Plan Aplanachromat 100× NA 1.4), with digital zooms of 0.7–1.3.

Intestinal Motility

Full thickness segments (1 cm) of terminal ileum and proximal colon were mounted in organ baths (3 ml) in physiological saline solution (mM: 118 NaCl, 4.8 KCl, 2.5 NaHCO₃, 1.0 NaH₂PO₄, 1.2 MgSO₄, 11.1 D-Glucose, 2.5 CaCl₂) under 1 g tension (37°C, 5% CO₂/95% O₂). Longitudinal contractions were recorded using isotonic transducers, and data were processed using an analog-to-digital converter (MP100, Biopac Systems, Inc., Goleta, CA), and analyzed using AcqKnowledge software (v3.7.3, Biopac). Tissues were equilibrated for 30 min, and challenged with carbachol (1 μM) to assess viability. Tissues were washed and challenged with DCA, TDCA, UDCA (1–100 μM) or vehicle (0.1% ethanol or distilled H₂O). The mean amplitude of the basal tension and the frequency of phasic contractions were determined 5 min before and after challenge. In some experiments, tissues were preincubated with atropine (1 μM, 10 min), hexamethonium (10 μM, 10 min), N-Nitro-L-Arginine Methyl Ester (L-NAME, 300 μM, 30 min) or with tetrodotoxin (1 μM, 5 min) (all from Sigma-Aldrich) prior to challenge with BAs.

Gastric emptying and small intestinal transit

Mice were fasted overnight with free access to water. Phenol red (0.07% in 0.9% NaCl) alone (control) or containing 0.03 M DCA or UDCA was administered by gavage (0.25 ml). After 30 min, mice were killed, the stomach and small intestine were removed, and the small intestine was divided into 3 equal segments. Tissues were homogenized with 0.5 ml of 0.1 N NaOH and 5.5 ml of H₂O, and centrifuged. Supernatant (1.5 ml) was mixed with 0.15 ml of trichloroacetic acid (30% w/v) to precipitate proteins, and centrifuged. Supernatants (1 ml) were mixed with NaOH (1 ml) and absorbance was measured at 570 nm and compared to a standard curve. Gastric emptying was determined as the proportion of administered phenol red remaining in the stomach after 30 min, using the formula: % gastric emptying = [(administered phenol red – gastric phenol red) / administered phenol red] × 100. Small intestinal transit was evaluated as geometric center of the distribution of the marker according to the following equation: geometric center = [Σ (phenol red in each segment) × (segment number)] / administered phenol red.

Statistical data analysis

Data are presented as mean ± SEM and were analyzed using one-way ANOVA with Newman-Keul's or Dunnett's multiple comparison tests. P<0.05 was considered significant.

RESULTS

GpBAR1 is a functional receptor when expressed in HEK cells

To verify that the cloned GpBAR1 receptor was functional, we measured cAMP generation in response to BAs known to activate GpBAR1 (32). The primary BAs, CDCA and CA, and the secondary BAs, TLCA, DCA and LCA, (100 μM) stimulated cAMP generation in HEK-GpBAR1-GFP cells (Fig. 1A). The potent GpBAR1 agonists TLCA and DCA had the largest effects, whereas UDCA, which activates GpBAR1 with low affinity, was less active. The effects of TLCA, LCA and DCA were concentration-dependent (10 nM - 100 μM, not shown). BAs did not stimulate cAMP generation in HEK-VC cells, and vehicle (0.1% ethanol) was without effect. Thus, HEK-GpBAR1-GFP cells express a functional BA receptor. These cells were used to characterize the GpBAR1 antibody.

Specificity of the GpBAR1 antibody

We evaluated specificity of the GpBAR1 antibody by immunofluorescence and Western blotting. In HEK-GpBAR1-GFP cells, the GFP signal completely colocalized with GpBAR1-IR at the plasma membrane and in vesicles (Fig. 1B). Preadsorption of the GpBAR1 antibody with the immunizing peptide abolished GpBAR1-IR, whereas the GFP signal was unaffected. GpBAR1-IR and GFP were not detected in HEK-VC cells. In membranes prepared from HEK-GpBAR1-GFP cells, the GFP and the GpBAR1 antibodies detected proteins with apparent molecular masses of ~65–70 kDa (Fig. 1C). The predicted molecular mass of the GpBAR1-GFP fusion protein is ~65 kDa (GpBAR1 ~35 kDa, GFP ~30 kDa). There are also two sites for potential N-linked glycosylation, which may account for the larger forms. Smaller proteins detected by GFP and GpBAR1 antibodies may represent degradation products. Preadsorption with immunizing peptide had no effect on GFP-IR signals but markedly reduced signals for GpBAR1-IR, with the exception of an unidentified protein at ~80 kDa. In HEK-VC cells, there were no detectable signals for GFP-IR, and GpBAR1-IR signals were markedly diminished. Thus, the GpBAR1 antibody specifically interacts with human GpBAR1.

GpBAR1-IR and mRNA are widely expressed in the gastrointestinal tract

We localized GpBAR1-IR in the mouse stomach and intestine by indirect immunofluorescence. GpBAR1-IR was most prominently detected in myenteric ganglia of the gastric corpus and antrum (Fig. 2a). There was no staining of the gastric mucosa or musculature. In the small and large intestine, GpBAR1-IR was detected in the enteric ganglia, *muscularis externa* and the mucosa (Fig. 2b). The relative intensities of the GpBAR1-IR signals consistently differed depending on the region. In all regions of small and large intestine, GpBAR1-IR was mainly localized to the enteric ganglia of the myenteric and submucosal plexuses. In the small intestine, GpBAR1-IR was also detected in the *muscularis externa* and in the mucosa, where GpBAR1-IR was present in enterocytes of the crypts and villi and in unidentified cells in the lamina propria. In the cecum and colon, GpBAR1-IR was detected at lower levels in the muscle and mucosa, and was more prominently detected in the enteric ganglia. In all segments, preadsorption of GpBAR1 antibody abolished staining (Fig. 2), and no staining was observed when the primary antibody was omitted (not shown). We examined expression of GpBAR1 mRNA in mouse gastrointestinal tissues by RT-PCR. A PCR product of the predicted size (449 bp) was amplified from gallbladder, liver, stomach, duodenum, ileum, cecum, and proximal and distal colon, but not from esophagus (Fig. 3). Analysis of dissected tissues indicated expression of GpBAR1 mRNA in the *muscularis externa*-myenteric plexus and the submucosa-submucosal plexus of the small and large intestine. Thus, GpBAR1 is widely expressed throughout the gastrointestinal tract, particularly in enteric ganglia.

GpBAR1 is prominently expressed by inhibitory motor neurons

To identify cell types expressing GpBAR1, we simultaneously localized GpBAR1 and PGP9.5 (pan-neuronal marker), nitric oxide synthase (NOS, identifies inhibitory motor neurons and descending interneurons), neurofilament M (NFM, identifies intrinsic primary afferent neurons), choline acetyltransferase (ChAT, identifies excitatory cholinergic neurons), or glial fibrillary acidic protein (GFAP, identifies enteric glia) (33). We restricted this analysis to the intestine, where GpBAR1-IR was more highly expressed than in the stomach and where chemical coding of enteric neurons is well established. Since GpBAR1-IR was more prominent in the myenteric than the submucosal plexus, quantification of neurons coexpressing marker proteins was restricted to the myenteric plexus (Table 2).

Myenteric plexus—Within myenteric ganglia of the small and large intestine, all cells expressing GpBAR1-IR coexpressed PGP9.5, and between 43% (ileum) and 52% (proximal colon) of PGP9.5-positive neurons coexpressed GpBAR1-IR (Fig. 4). Between 35% (duodenum) and 59% (distal colon) of neurons expressing GpBAR1-IR coexpressed NOS, and most NOS-positive neurons coexpressed GpBAR1-IR (84% duodenum, 90% distal colon) (Fig. 5). A variable proportion of GpBAR1-IR-positive neurons coexpressed NFM (23% duodenum, 57% distal colon, not shown) and ChAT (68% ileum, 28% distal colon, not shown). This variability may reflect differences in the proportion of different classes of neurons in these tissues. The colocalization of GpBAR1-IR and GFAP in glial cells was too infrequent to quantify, although colocalization was more apparent in the large intestine than the small intestine (Supplemental Fig. 1). Thus, GpBAR1-IR is almost exclusively expressed in neurons rather than glial cells of the myenteric plexus, where it is present in approximately half of all neurons. Nearly all NOS-positive neurons express GpBAR1-IR and a major proportion of GpBAR1-IR neurons express NOS and are inhibitory motor neurons or descending interneurons.

Submucosal plexus—Nearly all submucosal neurons expressing PGP9.5 coexpressed GpBAR1-IR in the small and large intestine (Fig. 6A). Approximately half of these GpBAR1-positive neurons coexpressed ChAT-IR (Fig. 6B). Although these neurons were

not further characterized, the detection of GpBAR1 in submucosal neurons suggests a role for this receptor in regulation of mucosal secretion.

In whole mounts of the myenteric and submucosal plexuses, preadsorption of GpBAR1 antibody abolished staining (Fig. 4).

GpBAR1 activation inhibits intestinal contractility

The localization of GpBAR1-IR in myenteric neurons suggests that this receptor may mediate effects of BAs on intestinal motility. Therefore, we examined the effects of BAs on contractility of longitudinal muscle of the small and large intestine. The potent GpBAR1 agonist DCA (32) caused a concentration-dependent (1–100 μ M) inhibition of spontaneous, phasic contractions of ileum (not shown) and proximal colon (Fig. 7A–B). The degree of inhibition was far greater in the proximal colon (Fig. 7C) than the ileum (Fig. 7D). The low affinity GpBAR1 agonist UDCA (100 μ M) (32), which retains the detergent properties of DCA, had a minor effect compared to DCA (Fig. 7A,C,D). The effects of the potent GpBAR1 agonist TDCA were examined in the ileum. TDCA (100 μ M) did not significantly alter the amplitude or frequency of spontaneous contractions relative to pretreatment values (Fig 7D). Tetrodotoxin (1 μ M, 5 min) and L-NAME (300 μ M, 30 min) abolished DCA-induced inhibition of motility in the ileum and proximal colon (Fig. 7A,C,D). The inhibitory effects of DCA on the proximal colon were significantly reduced by hexamethonium (10 μ M, 10 min), but not by atropine (1 μ M, 10 min) (Fig. 7C). Thus DCA, a potent GpBAR1 agonist, inhibits intestinal motility by a neurogenic, cholinergic and nitrergic mechanism that is consistent with the prominent localization of GpBAR1 to inhibitory motor neurons and ChAT-IR cholinergic neurons.

GpBAR1 activation delays gastric emptying and small intestinal transit

To determine whether lumenally-administered BAs affect gastrointestinal transit in mice, we administered DCA, UDCA or vehicle (control) by gavage. We assessed gastric emptying and small intestinal transit of phenol red. Compared to control mice treated with vehicle, DCA significantly delayed gastric emptying (Fig. 8A) and small intestinal transit (Fig. 8B,C). Within 30 min of phenol red administration to control mice, gastric emptying was 54.3%, and 14% of the marker was in the distal third segment of the small intestine (geometric center 2.7). In mice treated with DCA, gastric emptying was decreased by ~2-fold, 81.4% of the marker was in the first intestinal segment, 18.6% of the marker was in the second segment, and marker was absent from the third intestinal segment (geometric center 2.2). UDCA did not affect gastric emptying or small intestinal transit compared to control. Thus, luminal administration of a BA that activates GpBAR1 inhibits gastric emptying and small intestinal transit in mice.

DISCUSSION

We report the unexpected localization of GpBAR1-IR in myenteric and submucosal neurons of the mouse intestine. A large proportion of GpBAR1-expressing neurons of the myenteric plexus coexpressed NOS and are thus inhibitory motor neurons or descending interneurons, and the majority of these neurons expressed GpBAR1-IR. Consistent with this localization, a BA that is a potent GpBAR1 agonist inhibited motility of intestinal segments by a neurogenic, nitrergic mechanism, and delayed gastric emptying and intestinal transit. Our results reveal a novel function for BAs and GpBAR1 in the enteric nervous system, and provide a mechanistic explanation for the well-known actions of BAs on intestinal motility.

We detected GpBAR1-IR and mRNA throughout the gastrointestinal tract, with distinct regional differences. GpBAR1 mRNA was highly expressed in the mouse gall bladder, liver

and small and large intestine, including separated *muscularis externa*-myenteric plexus and submucosa-submucosal plexus. Lower levels were detected in the stomach and GpBAR1 was undetectable in the esophagus. These results agree with GpBAR1 mRNA expression in human tissues (13). We observed regional differences in GpBAR1-IR in the small and large intestine, with prominent localization in the mucosa and muscularis externa of the small intestine but not the colon. Although GpBAR1-IR was present in enterocytes of the small intestine, it was also present in unidentified cells in the lamina propria that may be macrophages or monocytes (12). We did not detect GpBAR1-IR in the colonic mucosa, which agrees with its lack of expression in colonic epithelial cell lines (13). However, GpBAR1 mRNA is present in cell lines derived from intestinal endocrine cells, where activation stimulates hormone release (13,19). It will be important to determine whether GpBAR1 is present in endocrine cells of the small and large intestine, where activation could control the secretion of hormones that regulate motility and gall bladder contraction.

The major unexpected finding of our study is the prominent localization of GpBAR1 in enteric neurons. GpBAR1-IR was present in approximately half of all myenteric neurons of the intestine. Within the myenteric plexus, most NOS-positive inhibitory neurons (>80%) expressed GpBAR1-IR, and a high proportion of GpBAR1-positive neurons coexpressed NOS, especially in the large intestine (49–60%). Detection of GpBAR1-IR in NOS-positive inhibitory neurons of the myenteric plexus suggests that these neurons mediate the inhibitory actions of BAs on intestinal motility. Supporting this suggestion, DCA, a potent agonist of GpBAR1, strongly inhibited spontaneous contractions of longitudinal muscle from the proximal colon, whereas UDCA, a weak agonist, had little effect. Although DCA inhibited contractions of the proximal colon and the ileum, the effect was far more marked in the colon. This difference is unlikely to reflect the minor differences in the proportion of GpBAR1-IR neurons coexpressing inhibitory or excitatory transmitters between the proximal colon and the ileum. A more likely explanation is the presence of GpBAR1-IR in muscle cells of the ileum but not the colon, allowing BAs to directly affect ileal muscle. In both tissues, tetrodotoxin and L-NAME abolished the effects of DCA. BAs also inhibit contractions of isolated rabbit and guinea pig ileum (29,30). Our results are consistent with the novel hypothesis that BAs activate GpBAR1 on inhibitory motor neurons to release NO, which inhibits spontaneous contractions of the intestine. This may represent a physiologically important mechanism, since luminal administration of DCA also inhibited gastric emptying and delayed intestinal transit in intact mice. The source of NO produced cannot be directly determined using our current methodology, and it may originate from non-neuronal cells (34). Although bile acids can activate muscarinic receptors (35), our data demonstrating that DCA-evoked inhibitory effects on contractile activity were unaffected by atropine indicates that muscarinic receptors are not involved in these responses. BAs may also act on the mucosa to release factors that control motility. The possibility that bile acids mediate their effects through a GpBAR1-independent mechanism can only be directly examined once GpBAR1-specific antagonists and GpBAR1-deficient mice become readily available.

Our findings may explain the well-known effects of luminal BAs on intestinal motility. BA infusion into the human jejunum or ileum inhibits transit, suggesting the existence of intestinal BA receptors (26,27). Thus, BAs may contribute to the “ileal brake”, by which BAs and lipids slow transit to permit complete digestion and absorption (27,36). Our observations that GpBAR1-IR is expressed by inhibitory motor neurons, and that a GpBAR1 agonist inhibits contractions by a neurogenic mechanism and delays transit, suggest that GpBAR1 mediates the ileal brake. Studies of GpBAR1-deficient mice are required to further evaluate this possibility. The mechanism by which luminal BAs activate neuronal GpBAR1 also remains to be determined. Luminal BAs could be transported across the epithelium through specific bile acid transporters to activate GpBAR1 on enteric nerve fibers or smooth

muscle cells (37), through a similar mechanism to that through which glucose affects myenteric neurons (38). The more hydrophobic bile acids, DCA and CDCA can more readily traverse the apical and basolateral plasma membrane bilayers (39), thereby, theoretically crossing the epithelium to reach submucosal or myenteric neurons. The inability of TDCA to inhibit contractile activity of the isolated ileum suggests that this hydrophilic bile acid does not effectively access target neurons within the small intestine. Luminal BAs may also affect the release of hormones from entero-endocrine cells, since hormonal mechanisms may also account for the BA-induced ileal brake (29). Alternatively, BAs from the circulation may activate the receptor on enteric neurons or other cell types. GpBAR1-IR was colocalized with NFM-IR, which has been characterized as a marker of IPANs in the mouse small intestine (33). IPANs innervate the mucosa and other neurons within the enteric circuitry (40), thus it is possible that BAs mediate their effects through specific activation of these neurons.

We detected GpBAR1-IR in intestinal submucosal neurons, many of which contain ChAT and are cholinergic secretomotor neurons or intrinsic primary afferent neurons (33). It remains to be determined if non-cholinergic secretomotor neurons containing vasoactive intestinal peptide also express GpBAR1. BAs stimulate secretion of fluid and mucus by a neuronal, cholinergic mechanism (20–22), which may also depend on NO generation (41). Our localization of GpBAR1-IR to cholinergic submucosal neurons raises the possibility that GpBAR1 mediates these effects of BAs on intestinal secretion. Thus, GpBAR1-expressing secretomotor neurons might function as chemo-sensors, stimulating secretory reflexes as a defensive mechanism to eliminate BAs and other noxious agents. However, BAs may directly activate GpBAR1 or other bile acid receptors on enterocytes to regulate fluid and electrolyte secretion. Activation of GpBAR1 in the gall bladder epithelium stimulates the cystic fibrosis transmembrane conductor regulator chloride channel to promote chloride secretion (14). Additional studies are required to define the role of GpBAR1 in BA-induced secretion in the intestine.

In conclusion, we have described the unique localization of the BA receptor GpBAR1 in the enteric nervous system, where the receptor is suitably located to mediate the effects of BAs on intestinal motility and secretion. This report adds to the emerging role of GpBAR1 in control of energy expenditure, weight gain, blood flow, bile acid homeostasis and immune responses.

Supplementary Material

Refer to Web version on PubMed Central for supplementary material.

Acknowledgments

Supported by grants from the Northern California Institute for Research and Education, the Veterans Health Administration and NIH DK026743 (CUC), from NIH DK07573 (JCP, NWB), DK39957, DK43207 and DK57840 (NWB), NH&MRC 454858 CJ Martin Fellowship (DPP) and a Neurogastroenterology and Motility Meeting 2009 Young Investigator Travel Award (DPP).

REFERENCES

1. Monte MJ, Marin JJ, Antelo A, Vazquez-Tato J. Bile acids: chemistry, physiology, and pathophysiology. *World J Gastroenterol.* 2009 Feb 21; 15(7):804–816. [PubMed: 19230041]
2. Keitel V, Kubitz R, Haussinger D. Endocrine and paracrine role of bile acids. *World J Gastroenterol.* 2008 Oct 7; 14(37):5620–5629. [PubMed: 18837077]
3. Lefebvre P, Cariou B, Lien F, Kuipers F, Staels B. Role of bile acids and bile acid receptors in metabolic regulation. *Physiol Rev.* 2009 Jan; 89(1):147–191. [PubMed: 19126757]

4. Claudel T, Staels B, Kuipers F. The Farnesoid X receptor: a molecular link between bile acid and lipid and glucose metabolism. *ArteriosclerThrombVascBiol.* 2005; 25(10):2020–2030.
5. Wang H, Chen J, Hollister K, Sowers LC, Forman BM. Endogenous bile acids are ligands for the nuclear receptor FXR/BAR. *MolCell.* 1999; 3(5):543–553.
6. Staudinger JL, Goodwin B, Jones SA, Hawkins-Brown D, MacKenzie KI, LaTour A, et al. The nuclear receptor PXR is a lithocholic acid sensor that protects against liver toxicity. *ProcNatlAcadSciUSA.* 2001; 98(6):3369–3374.
7. Makishima M, Lu TT, Xie W, Whitfield GK, Domoto H, Evans RM, et al. Vitamin D receptor as an intestinal bile acid sensor. *Science.* 2002; 296(5571):1313–1316. [PubMed: 12016314]
8. Bouscarel B, Kroll SD, Fromm H. Signal transduction and hepatocellular bile acid transport: cross talk between bile acids and second messengers. *Gastroenterology.* 1999; 117(2):433–452. [PubMed: 10419927]
9. Gupta S, Stravitz RT, Dent P, Hylemon PB. Down-regulation of cholesterol 7 α -hydroxylase (CYP7A1) gene expression by bile acids in primary rat hepatocytes is mediated by the c-Jun N-terminal kinase pathway. *JBiolChem.* 2001; 276(19):15816–15822.
10. Looby E, Long A, Kelleher D, Volkov Y. Bile acid deoxycholate induces differential subcellular localisation of the PKC isoenzymes beta 1, epsilon and delta in colonic epithelial cells in a sodium butyrate insensitive manner. *IntJCancer.* 2005; 114(6):887–895.
11. Qiao L, Han SI, Fang Y, Park JS, Gupta S, Gilford D, et al. Bile acid regulation of C/EBPbeta, CREB, and c-Jun function, via the extracellular signal-regulated kinase and c-Jun NH2-terminal kinase pathways, modulates the apoptotic response of hepatocytes. *MolCell Biol.* 2003; 23(9): 3052–3066.
12. Kawamata Y, Fujii R, Hosoya M, Harada M, Yoshida H, Miwa M, et al. A G protein-coupled receptor responsive to bile acids. *J Biol Chem.* 2003 Mar 14; 278(11):9435–9440. [PubMed: 12524422]
13. Maruyama T, Miyamoto Y, Nakamura T, Tamai Y, Okada H, Sugiyama E, et al. Identification of membrane-type receptor for bile acids (M-BAR). *Biochem Biophys Res Commun.* 2002 Nov 15; 298(5):714–719. [PubMed: 12419312]
14. Keitel V, Cupisti K, Ullmer C, Knoefel WT, Kubitz R, Haussinger D. The membrane-bound bile acid receptor TGR5 is localized in the epithelium of human gallbladders. *Hepatology.* 2009 Apr 17.
15. Keitel V, Donner M, Winandy S, Kubitz R, Haussinger D. Expression and function of the bile acid receptor TGR5 in Kupffer cells. *Biochem Biophys Res Commun.* 2008 Jul 18; 372(1):78–84. [PubMed: 18468513]
16. Keitel V, Reinehr R, Gatsios P, Rupprecht C, Gorg B, Selbach O, et al. The G-protein coupled bile salt receptor TGR5 is expressed in liver sinusoidal endothelial cells. *Hepatology.* 2007 Mar; 45(3): 695–704. [PubMed: 17326144]
17. Maruyama T, Tanaka K, Suzuki J, Miyoshi H, Harada N, Nakamura T, et al. Targeted disruption of G protein-coupled bile acid receptor 1 (Gpbar1/M-Bar) in mice. *J Endocrinol.* 2006 Oct; 191(1): 197–205. [PubMed: 17065403]
18. Watanabe M, Houten SM, Mataki C, Christoffolete MA, Kim BW, Sato H, et al. Bile acids induce energy expenditure by promoting intracellular thyroid hormone activation. *Nature.* 2006 Jan 26; 439(7075):484–489. [PubMed: 16400329]
19. Katsuma S, Hirasawa A, Tsujimoto G. Bile acids promote glucagon-like peptide-1 secretion through TGR5 in a murine enteroendocrine cell line STC-1. *BiochemBiophysResCommun.* 2005; 329(1):386–390.
20. Camilleri M, Murphy R, Chadwick VS. Pharmacological inhibition of chenodeoxycholate-induced fluid and mucus secretion and mucosal injury in the rabbit colon. *DigDisSci.* 1982; 27(10):865–869.
21. Karlstrom L. Evidence of involvement of the enteric nervous system in the effects of sodium deoxycholate on small-intestinal transepithelial fluid transport and motility. *ScandJGastroenterol.* 1986; 21(3):321–330.

22. Karlstrom L, Cassuto J, Jodal M, Lundgren O. Involvement of the enteric nervous system in the intestinal secretion induced by sodium deoxycholate and sodium ricinoleate. *ScandJGastroenterol*. 1986; 21(3):331–340.
23. Feldman S, Gibaldi M. Effect of bile salts on gastric emptying and intestinal transit in the rat. *Gastroenterology*. 1968; 54(5):918–921. [PubMed: 5652526]
24. Kirwan WO, Smith AN, Mitchell WD, Falconer JD, Eastwood MA. Bile acids and colonic motility in the rabbit and the human. *Gut*. 1975; 16(11):894–902. [PubMed: 1193418]
25. Falconer JD, Smith AN, Eastwood MA. The effects of bile acids on colonic motility in the rabbit. *QJExpPhysiol Cogn MedSci*. 1980; 65(2):135–144.
26. Penagini R, Misiewicz JJ, Frost PG. Effect of jejunal infusion of bile acids on small bowel transit and fasting jejunal motility in man. *Gut*. 1988 Jun; 29(6):789–794. [PubMed: 3384363]
27. Penagini R, Spiller RC, Misiewicz JJ, Frost PG. Effect of ileal infusion of glycochenodeoxycholic acid on segmental transit, motility, and flow in the human jejunum and ileum. *Gut*. 1989 May; 30(5):609–617. [PubMed: 2731753]
28. Van Ooteghem NA, Van Erpecum KJ, Van Berge-Henegouwen GP. Effects of ileal bile salts on fasting small intestinal and gallbladder motility. *NeurogastroenterolMotil*. 2002; 14(5):527–533.
29. Armstrong DN, Krenz HK, Modlin IM, Ballantyne GH. Bile salt inhibition of motility in the isolated perfused rabbit terminal ileum. *Gut*. 1993 Apr; 34(4):483–488. [PubMed: 8491394]
30. Romero F, Frediani-Neto E, Paiva TB, Paiva AC. Role of Na⁺/Ca⁺⁺ exchange in the relaxant effect of sodium taurocholate on the guinea-pig ileum smooth muscle. *Naunyn Schmiedebergs ArchPharmacol*. 1993; 348(3):325–331.
31. Poole DP, Castelucci P, Robbins HL, Chiocchetti R, Furness JB. The distribution of P2X3 purine receptor subunits in the guinea pig enteric nervous system. *AutonNeurosci*. 2002; 101(1–2):39–47.
32. Sato H, Macchiarulo A, Thomas C, Gioiello A, Une M, Hofmann AF, et al. Novel potent and selective bile acid derivatives as TGR5 agonists: biological screening, structure-activity relationships, and molecular modeling studies. *J Med Chem*. 2008 Mar 27; 51(6):1831–1841. [PubMed: 18307294]
33. Qu ZD, Thacker M, Castelucci P, Bagyzanski M, Epstein ML, Furness JB. Immunohistochemical analysis of neuron types in the mouse small intestine. *Cell Tissue Res*. 2008; 334(2):147–161. [PubMed: 18855018]
34. Khurana S, Yamada M, Wess J, Kennedy RH, Raufman JP. Deoxycholytaurine-induced vasodilation of rodent aorta is nitric oxide- and muscarinic M(3) receptor-dependent. *Eur J Pharmacol*. 2005 Jul 4; 517(1–2):103–110. [PubMed: 15964566]
35. Raufman JP, Cheng K, Zimniak P. Activation of muscarinic receptor signaling by bile acids: physiological and medical implications. *Dig Dis Sci*. 2003 Aug; 48(8):1431–1444. [PubMed: 12924634]
36. Spiller RC, Trotman IF, Higgins BE, Ghatei MA, Grimble GK, Lee YC, et al. The ileal brake--inhibition of jejunal motility after ileal fat perfusion in man. *Gut*. 1984; 25(4):365–374. [PubMed: 6706215]
37. Dawson PA, Lan T, Rao A. Bile acid transporters. *J Lipid Res*. 2009 Dec; 50(12):2340–2357. [PubMed: 19498215]
38. Liu M, Seino S, Kirchgessner AL. Identification and characterization of glucoresponsive neurons in the enteric nervous system. *J Neurosci*. 1999 Dec 1; 19(23):10305–10317. [PubMed: 10575028]
39. Cabral DJ, Small DM, Lilly HS, Hamilton JA. Transbilayer movement of bile acids in model membranes. *Biochemistry*. 1987 Apr 7; 26(7):1801–1804. [PubMed: 3593691]
40. Furness JB, Jones C, Nurgali K, Clerc N. Intrinsic primary afferent neurons and nerve circuits within the intestine. *Prog Neurobiol*. 2004 Feb; 72(2):143–164. [PubMed: 15063530]
41. Mascolo N, Gagarella TS, Izzo AA, Di CG, Capasso F. Nitric oxide involvement in sodium choleate-induced fluid secretion and diarrhoea in rats. *EurJPharmacol*. 1994; 264(1):21–26.

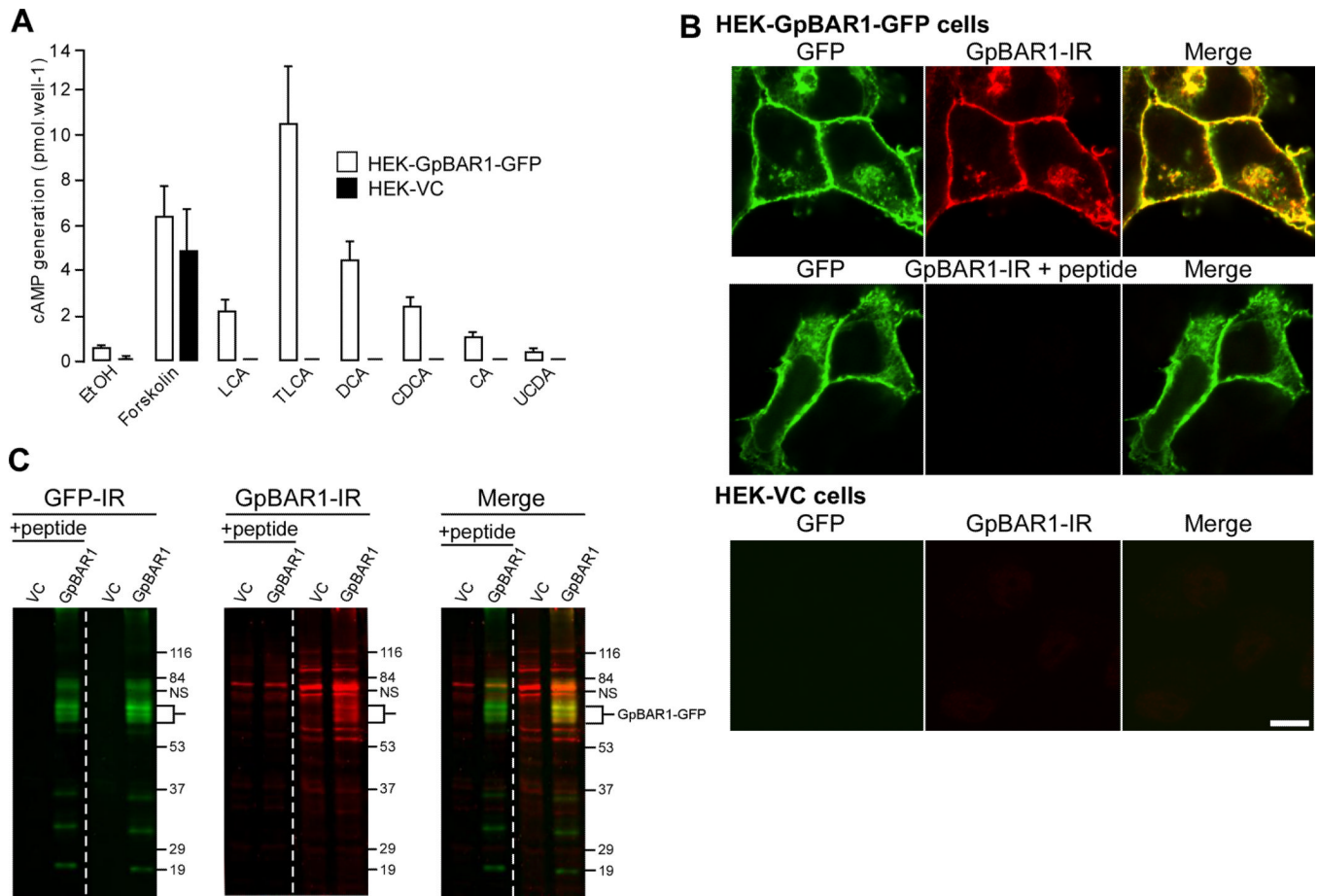


Figure 1. GpBAR1 antibody characterization

A. BA-stimulated cAMP generation. HEK-GpBAR1-GFP and HEK-VC cells were incubated with vehicle (0.1% ethanol, EtOH), forskolin (10 nM) or BAs (100 μM) for 5 min. cAMP generation is expressed in pmol per well (n=6). **B.** Localization of GpBAR1-IR by immunofluorescence. In HEK-GpBAR1-GFP cells, GFP and GpBAR1-IR colocalized at the plasma membrane and in vesicles (upper row). Preadsorption (+ peptide) abolished signal for GpBAR1-IR but not GFP (middle row). Neither GFP nor GpBAR1-IR was detected in HEK-VC cells (bottom row). Scale bar = 10 μm. **C.** Detection of GpBAR1-IR by Western blotting. Membranes from HEK-GpBAR1-GFP or HEK-VC cells were separated by SDS-PAGE. The same blot was probed with antibodies to GFP (left) or GpBAR1 (middle) (right lanes) or preadsorbed antibody to GpBAR1 (left lanes, + peptide). Merged images are in right panel. In membranes from HEK-GpBAR1-GFP cells, antibodies to GFP and GpBAR1 detected proteins of ~60–70 kDa, corresponding to the GpBAR1-GFP fusion protein (merged). In membranes from HEK-VC cells, GFP-IR was undetectable and GpBAR1-IR was markedly diminished. Preadsorption of GpBAR1 antibody did not affect GFP-IR but suppressed GpBAR1-IR.

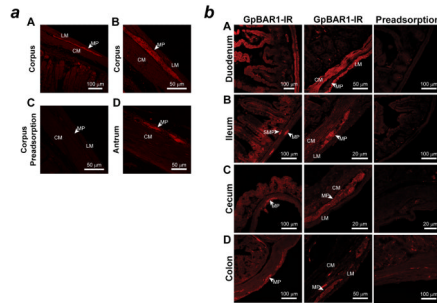


Figure 2. Localization of GpBAR1-IR in sections of mouse stomach and small and large intestine
a: Representative examples of GpBAR1-IR in the wall of the gastric corpus (**A**, **B**, **C**) and antrum (**D**). GpBAR1-IR was expressed in the myenteric plexus (MP). Circular muscle, CM; longitudinal muscle, LM. Preadsorption of the GpBAR1 antibody with immunizing peptide abolished GpBAR1-IR (**C**).
b: Representative examples of GpBAR1-IR in the wall of the duodenum (**A**), ileum (**B**), cecum (**C**) and colon (**D**) are shown. GpBAR1-IR was expressed in the myenteric plexus (MP) and submucosal plexus (SMP) of the small and large intestine. GpBAR1-IR was more highly expressed in the mucosa, *muscularis externa* (circular muscle, CM; longitudinal muscle, LM), of the small intestine compared to the large intestine. Preadsorption of the GpBAR1 antibody with immunizing peptide abolished GpBAR1-IR.

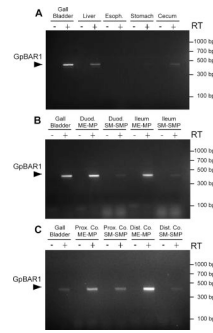


Figure 3. Amplification of GpBAR1 mRNA in gastrointestinal tissues

A 449 bp product corresponding to GpBAR1 was amplified and identified by sequence analysis. **A.** GpBAR1 was amplified from gall bladder, liver and cecum, with low levels in stomach and no detectable product in esophagus (Esoph.). **B, C.** GpBAR1 was highly expressed in dissected *muscularis externa*-myenteric plexus (ME-MP) and expressed at lower levels in dissected submucosa-submucosal plexus (SM-SMP) of duodenum (Duod.), ileum, proximal colon (Prox. Co.) and distal colon (Dist. Co.). No products were detected without reverse transcriptase (RT).

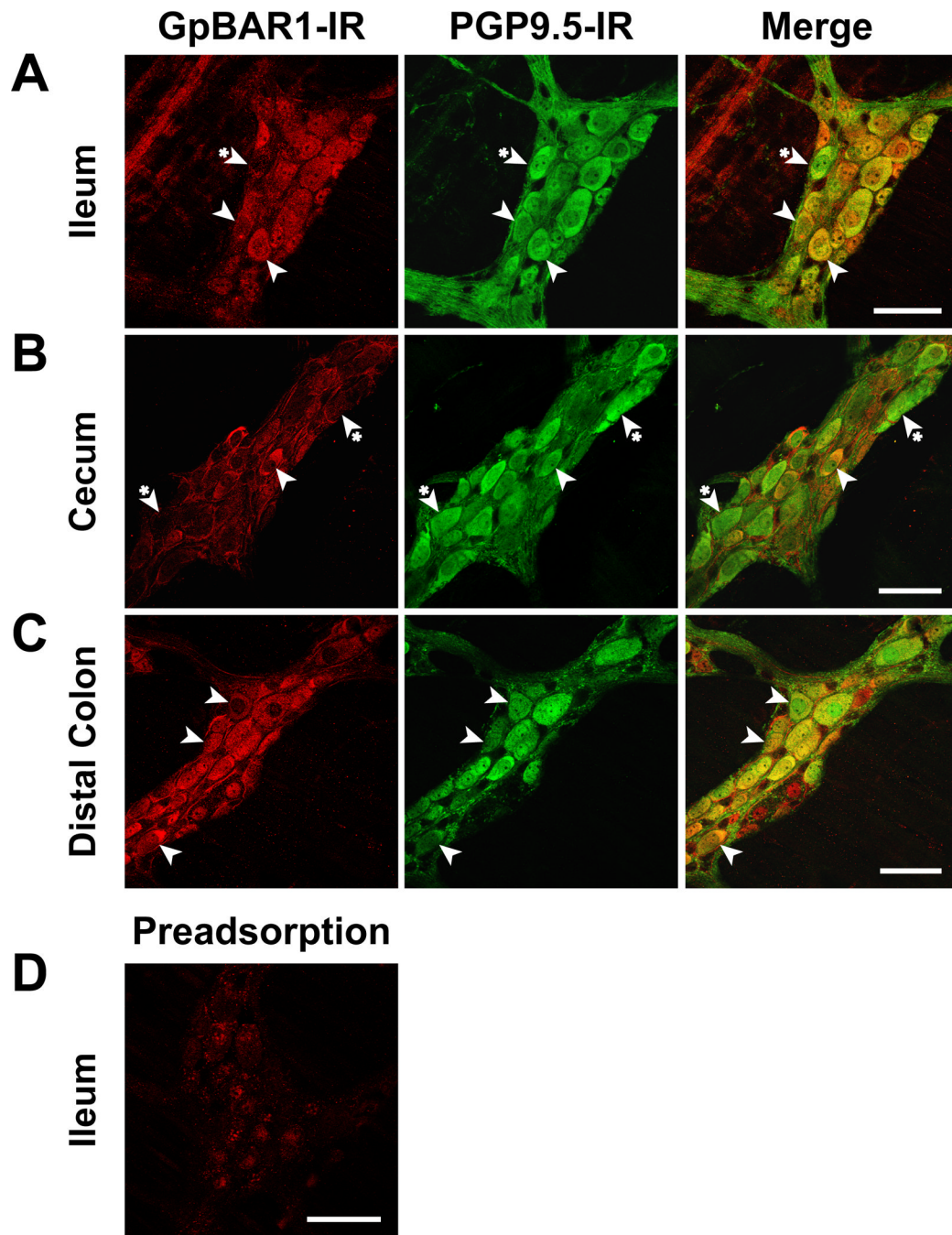


Figure 4. Localization of GpBAR1-IR and PGP9.5-IR in whole mounts of myenteric plexus GpBAR1-IR (left panels) was detected in approximately half of all myenteric neurons expressing PGP9.5-IR (middle panels) in the ileum (**A**), cecum (**B**) and distal colon (**C**). Merged images (right panels) demonstrate colocalization of GpBAR1-IR and PGP9.5-IR (arrowheads). Although cells expressing GpBAR1-IR almost always expressed PGP9.5-IR, some PGP9.5-IR positive neurons did not express GpBAR1-IR (arrowheads with asterisk). **D.** PreadSORption of the GpBAR1 antibody with immunizing peptide abolished GpBAR1-IR in the ileum. Scale bars = 50 μ m.

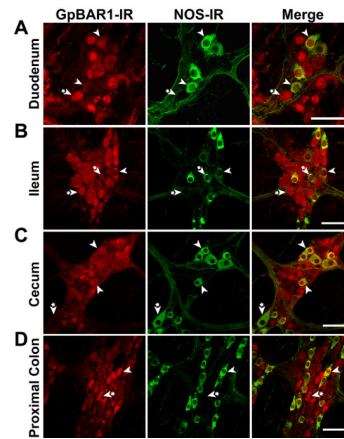


Figure 5. Localization of GpBAR1-IR and NOS-IR in whole mounts of myenteric plexus
 Most (>80%) neurons expressing GpBAR1-IR (left panels) also expressed NOS-IR (middle panels) in the duodenum (**A**), ileum (**B**), cecum (**C**) and proximal colon (**D**). Merged images (right panels) demonstrate colocalization of GpBAR1-IR and NOS-IR (arrowhead). Neurons expressing only GpBAR1-IR or NOS-IR are indicated (arrowheads with asterisk). Scale bars = 50 μ m.

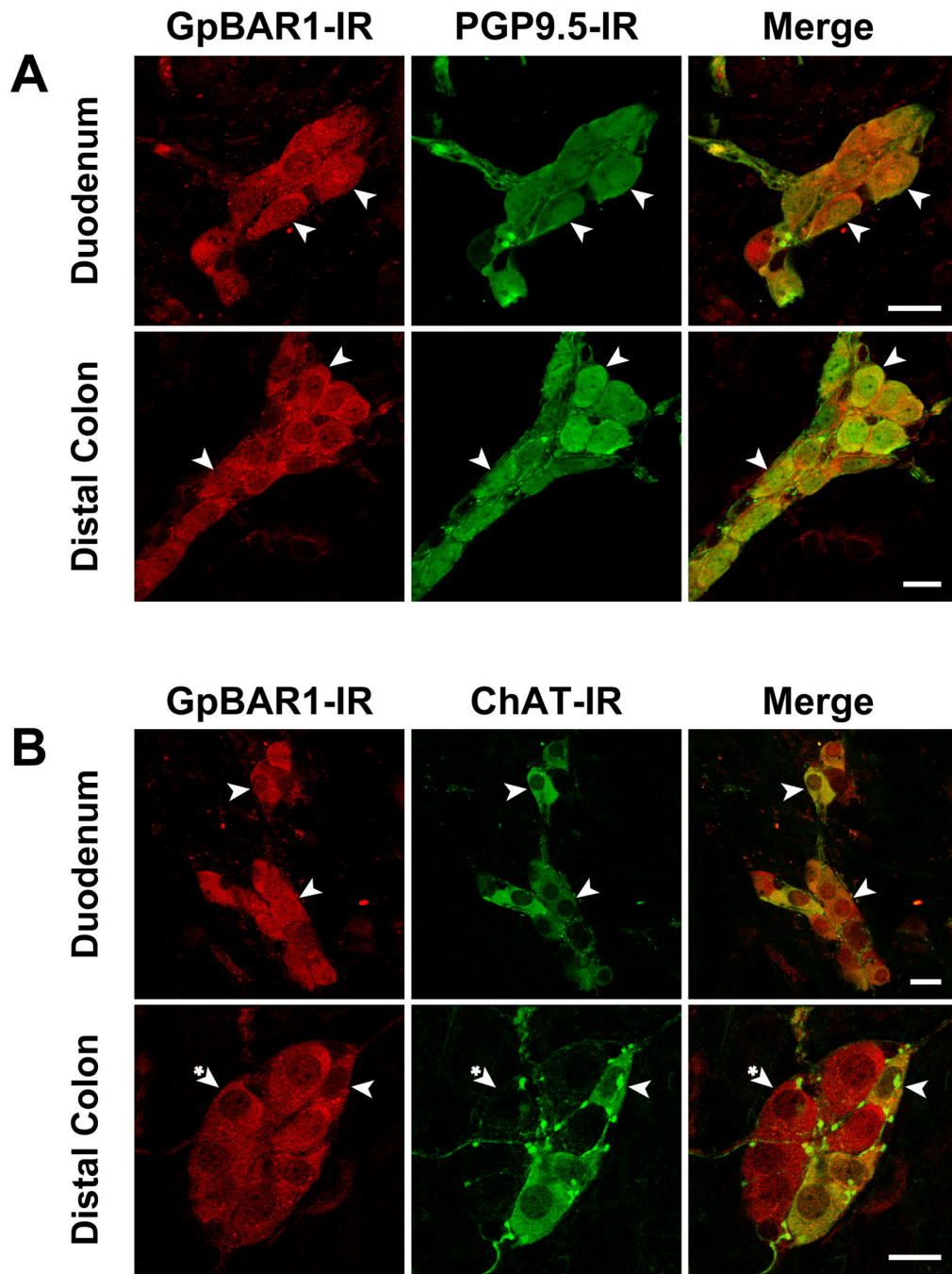


Figure 6. Localization of GpBAR1-IR, PGP9.5-IR and ChAT-IR in whole mounts of submucosal plexus

Localization of GpBAR1-IR (left panels) and PGP9.5-IR (middle panels) (A) or ChAT-IR (middle panels) (B) in duodenum and distal colon. Merged images (right panels) indicate invariable colocalization of GpBAR1-IR and PGP9.5-IR, and frequent colocalization of GpBAR1-IR and ChAT-IR (arrowheads). Some neurons expressing GpBAR1-IR did not express ChAT-IR (arrowheads with asterisk). Scale bars = 20 μ m.

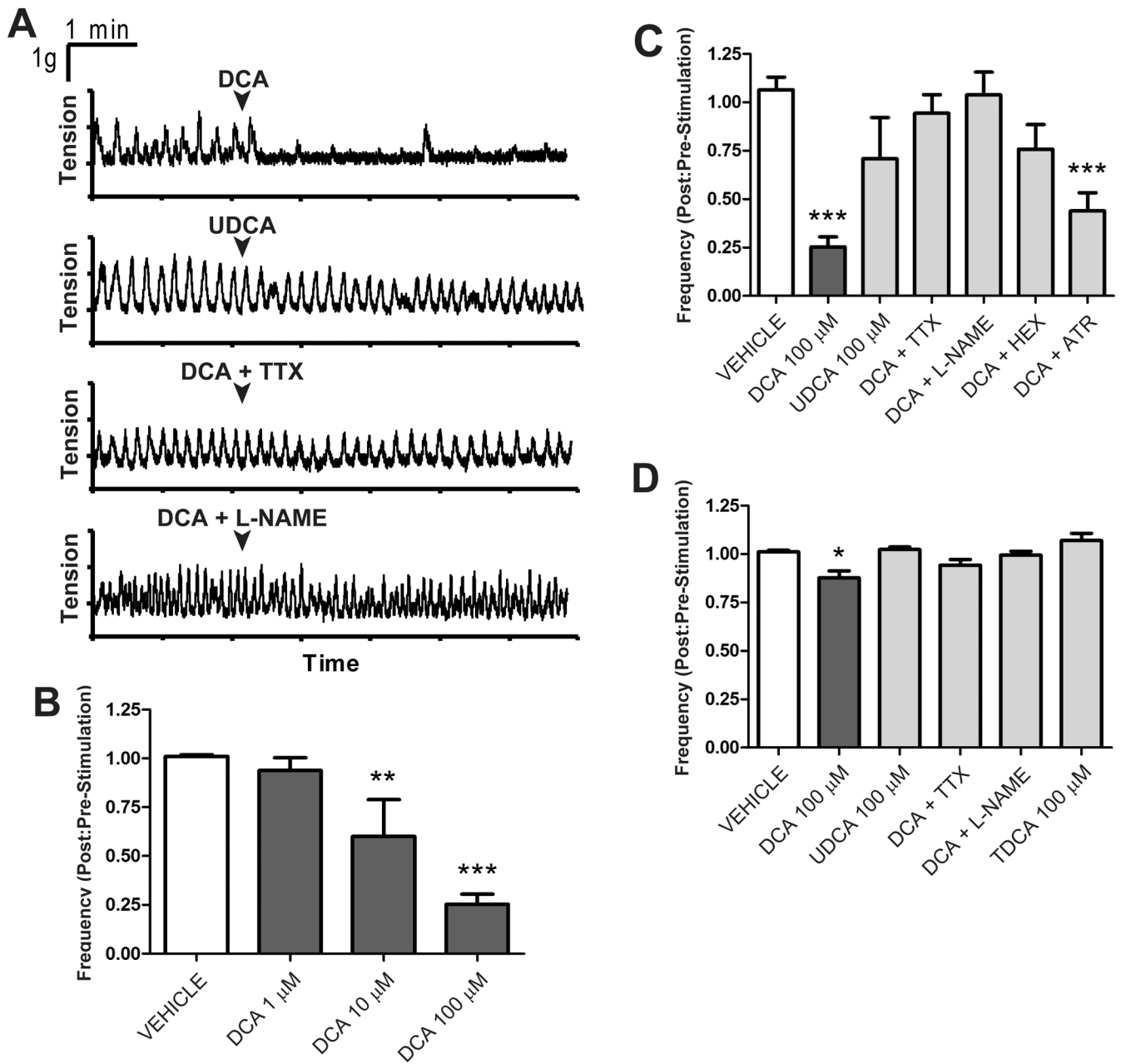


Figure 7. Effects of BAs on spontaneous contractile activity of longitudinal muscle of the proximal colon and ileum

A. Representative recordings from proximal colon. DCA (100 μ M) immediately inhibited spontaneous phasic contractions, but did not alter basal tone. UDCA (100 μ M) did not reduce the frequency of spontaneous contractions. Tetrodotoxin (TTX) and L-NAME abolished the effects of DCA. **B–D.** Effects of treatments on frequency of contraction, in which the frequency prior to stimulation is normalized to 1. **B.** Effects of graded concentrations on DCA in proximal colon. **C, D.** Tetrodotoxin and L-NAME abolished the effects of DCA in the proximal colon (**C**) and ileum (**D**). The effects of DCA (100 μ M) on the proximal colon were significantly reduced by hexamethonium, but not by atropine (**C**). TDCA (100 μ M) did not have any effect on spontaneous activity of the ileum relative to vehicle control (**D**). * $P < 0.05$, ** $P < 0.01$, *** $P < 0.001$ ($n \geq 6$).

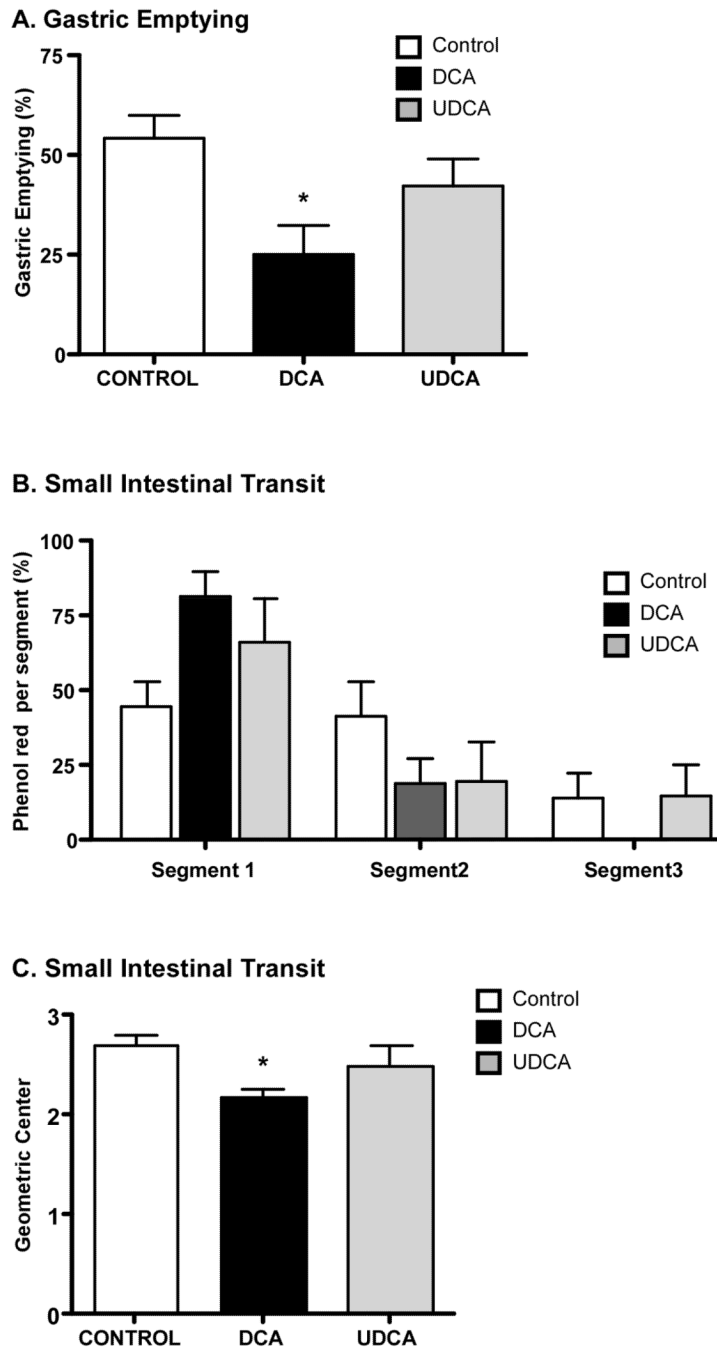


Figure 8. Effects of BAs on gastric emptying and small intestinal transit
 Phenol red and DCA, UCDA or vehicle (control) were administered by gavage. After 30 min, the proportion of the administered phenol red was determined in the stomach and in 3 equal segments of small intestine. Gastric emptying (A), transit of the marker in the intestinal segments (B) and the geometric center of the marker in the small intestine (C) were determined. Compared to control, DCA but not UCDA inhibited gastric emptying and caused retention of the marker in the proximal segments of the intestine, reducing the geometric mean of the marker distribution. * $P < 0.05$ ($n \geq 6$).

Table 1

Sources and dilutions of primary antibodies.

Antigen	Species	Conditions	Source
GpBAR1	Rabbit	IF/WB, 1:100	
GFP	Mouse	WB 1:10,000	Santa Cruz Biotechnology, Santa Cruz, CA
ChAT	Goat	IF, 1:200	Millipore, Temecula, CA
GFP	Mouse	IF/WB, 1:10,000	Santa Cruz Biotechnology, Santa Cruz, CA
GFAP	Goat	IF, 1:400	NOVUS Biologicals, Littleton, CO
NFM	Chicken	IF, 1:500	Gene Tex Inc., Irvine, CA
NOS	Goat	IF, 1:500	NOVUS Biologicals, Littleton, CO
PGP9.5	Chicken	IF, 1:500	Abcam Inc., Cambridge, MA

IF, immunofluorescence; WB, Western blot.

Table 2

Quantification of neurons in myenteric plexus.

Region	PGP9.5	NOS	NFM	ChAT
Duodenum	^A 126/126 (100%) ^B 126/295 (43%)	52/147 (35%) 52/62 (84%)	3/52 (6%) 3/13 (23%)	60/157 (38%) 60/90 (67%)
Ileum	177/177 (100%) 177/425 (42%)	97/213 (46%) 97/114 (85%)	10/130 (8%) 10/26 (38%)	54/140 (39%) 54/79 (68%)
Cecum	102/102 (100%) 102/220 (46%)	158/265 (60%) 158/177 (89%)	24/103 (23%) 24/49 (49%)	35/85 (41%) 35/89 (39%)
Proximal Colon	175/175 (100%) 175/335 (52%)	106/216 (49%) 106/123 (86%)	13/110 (12%) 13/54(24%)	30/77 (39%) 30/74 (41%)
Distal Colon	113/113 (100%) 113/242 (47%)	140/255 (59%) 140/156 (90%)	21/128 (16%) 21/37 (57%)	32/133 (24%) 32/113 (28%)

For each region, the upper number^A indicates the number of marker-positive neurons in the GpBAR1-positive population (*i.e.* in duodenum, of 126 cells expressing GpBAR1, 126 expressed PGP9.5), and the lower number^B indicates the number of GpBAR1-positive cells in the marker-positive population (*i.e.* in duodenum, of 295 cells expressing PGP9.5, 126 expressed GpBAR1). For all regions, n≥3 mice.